Spatial regression models for extreme precipitation in Belgium

H. Van de Vyver[1]

[1] Quantification of precipitation extremes is important for flood planning purposes, and a common measure of extreme events is the T year return level. Extreme precipitation depths in Belgium are analyzed for accumulation durations ranging from 10 min to 30 days. Spatial generalized extreme value (GEV) models are presented by considering multisite data and relating GEV parameters to geographical/climatological covariates through a common regression relationship. Methods of combining data from several sites are in common use, and in such cases, there is likely to be nonnegligible intersite dependence. However, parameter estimation in GEV models is generally done with the maximum likelihood estimation method (MLE) that assumes independence. Estimates of uncertainty are adjusted for spatial dependence using methodologies proposed earlier. Consistency of GEV distributions for various durations is obtained by fitting a smooth function to the preliminary estimations of the shape parameter. Model quality has been assessed by various statistical tests and indicates the relevance of our approach. In addition, a methodology is applied to account for the fact that measurements have been made in fixed intervals (usually 09:00 UTC–09:00 UTC). The distribution of the annual sliding 24 h maxima was specified through extremal indices of a more than 110 year time series of 24 h aggregated 10 min rainfall and daily rainfall. Finally, the selected models are used for producing maps of precipitation return levels.

1. Introduction

[2] Extreme rainfall events have a large impact on society and can lead to loss of life and property, for example, by causing land slides or flooding due to dike breach or dam failures. Think for instance of the recent flood of November 2010 where the total damage in Belgium was estimated on 180 million euro. There are many situations in water resources systems in which the statistics of extremes plays a decisive role. Rainfall intensity patterns for various return periods are required for designing hydraulic structures or for flood mapping and zoning. Knowledge of the temporal and spatial distribution of these extreme events is thus of great practical importance. Extreme value theory is the branch of probability and statistics dedicated to characterizing the behavior of extreme observations. There are many excellent textbooks on this subject including those by *Leadbetter et al.* [1983] and *Embrechts et al.* [1997] which give a comprehensive mathematical background of the theory, and those by *Coles* [2001] and *Beirlant et al.* [2004] which focuses on applications and data analysis. The theory has been widely used in hydrology [*Jenkinson*, 1955; *Sneyers*, 1960; *Katz et al.*, 2002; *El Adlouni et al.*, 2007; *Ntegeka and Willems*, 2008; *Blanchet et al.*, 2009; *Overeem et al.*, 2009; *Ailliot et al.*, 2011] and other environmental sciences and finance as well.

[3] The generalized extreme value (GEV) distribution has been used in many studies and often provides a good fit to extreme rainfall maxima. It is well recognized that a satisfactory fit of the GEV distribution to a single record does not guarantee good estimates of large return period events. More data are required to get a reliable description of the extreme upper tail. The need for more data can be fulfilled by combining several data sets under a GEV model which assumes that one or more parameters are either common to all the locations or are related to covariates through a common regression relationship. An overview of early methods for regional frequency estimation is given by *Buishand* [1991]. One of the best known methodologies is the so-called regional index flood estimation [*Cunnane*, 1973; *Hosking and Wallis*, 1997], which is based on the hypothesis that data at different sites in the region follow the same distribution except for scale (index flood). However, most of these methods are based on the assumption of spatial independence, a condition which is usually not met in practical applications. This problem has been recognized, but for a long time no clear-cut solution has emerged. *Buishand* [1984] modeled explicitly spatial dependence based on bivariate GEV distributions. In recent years, there is a growing interest in spatial modeling of multivariate extremes based on maximum-stable processes [*Schlater*, 2002; R. L. Smith, Max-stable processes and spatial extremes, unpublished manuscript, 1990a], and exhaustive R packages on this topic have already been developed [*Ribatet*, 2011]. However, multivariate methodologies cannot address the problem if interest is in the marginal distribution. A satisfying approach to obtain maximum

---

[1]Royal Meteorological Institute of Belgium, Brussels, Belgium.

Corresponding author: H. Van de Vyver, Royal Meteorological Institute of Belgium, Ringlaan 3 Ave. Circulaire, B-1180 Brussels, Belgium. (hvijver@meteo.be)

likelihood estimates in regional GEV models under the artificial assumption that the series are independent has been formulated by R. L. Smith (Regional estimation from spatially dependent data, unpublished manuscript, 1990b). The likelihood function was constructed as if the sites were independent, but the error estimation and likelihood ratio test were adjusted to account for spatial correlation. Recent developments of spatial modeling in a Bayesian framework are given by *Cooley et al.* [2007]. All the above mentioned methodologies are based on direct estimation of the spatial extreme value distribution. Another important class, which is not the subject of this paper, is based on spatial interpolation of individual estimations. A comparative study of these two main approaches has been made by *Blanchet and Lehning* [2010].

[4] The spatial distribution of extreme precipitation in Belgium is analyzed by regression modeling and highlighting the regional variabilities. Although, studies on extreme precipitation in Belgium are numerous [*Sneyers*, 1960; *Demarée*, 1985; *Buishand and Demarée*, 1990; *Gellens*, 1995, 2000, 2002, 2003; *Willems*, 2000; *Delbeke*, 2001; *Vannitsem and Naveau*, 2007; *Ntegeka and Willems*, 2008], most of them are focused on single-site estimations. A great advantage of spatial models is that they apply at any place, even at ungauged sites.

[5] This article is organized as follows. In section 2 the principles of extreme value theory are recalled, and spatial extensions of the classical model are introduced. A brief data description and homogeneity testing of series are given in section 3. Assessment of spatial correlation and significance of regional variability of GEV parameters can be found in section 4. Spatial regression modeling of extremes based on multisite precipitation data is carried out in section 5. In addition, the models obtained are extensively validated. Section 6 is devoted to transforming the GEV parameters of daily (sampled at 09:00 UTC) maximum rainfall to those of 24 h (i.e., sampled at arbitrary time) maximum rainfall. Finally, in section 7, some conclusions are drawn.

2. Statistical Theory of Extreme Values

[6] The use of extreme value models is increasingly common in climate studies. These models are concerned with the statistical behavior of block maxima, i.e.,

$$M_m = \max\{X_1, \ldots, X_m\}, \tag{1}$$

where $X_1, \ldots, X_m$ is a sequence of independent and identically distributed (iid) random variables. In practice, $X_1, \ldots, X_m$ is, for instance, a time series of daily precipitation. Pragmatic considerations often led to the adoption of blocks of length 1 year.

2.1. Classical GEV Model

[7] Classical extreme value analysis is based on the assumption that $X_1, \ldots, X_m$ is a sequence of iid random variables. A key result is that in such a case the cumulative distribution of the normalized maxima converges to the generalized extreme value (GEV) distribution as $m \to \infty$, i.e.,

$$\lim_{m \to \infty} \Pr\{(M_m - b_m)/a_m \le y\} \to G_\gamma(y), \tag{2}$$

where the GEV distribution is of the form

$$G_\gamma(y) = \exp\left[-(1 + \gamma y)^{-1/\gamma}\right], \quad \text{if} \quad 1 + \gamma y > 0. \tag{3}$$

Here γ is called the shape parameter and governs how rapidly the upper tail decays. It is a key quantity in the whole of extreme value analysis. Note that the shape parameter $\kappa = -\gamma$ is often used in the hydrological literature. For notational convenience, denote the maximum of a sample $X_1, \ldots, X_m$ by Z. Then, for sufficiently large m the distribution of Z can be approximated by the three-parameter GEV distribution, $Z \sim GEV(\mu, \sigma, \gamma)$, with

$$G(z; \mu, \sigma, \gamma) = \exp\left[-\left(1 + \gamma \frac{z - \mu}{\sigma}\right)^{-1/\gamma}\right],$$
$$\text{if} \quad 1 + \gamma \frac{z - \mu}{\sigma} > 0, \tag{4}$$

where μ and $\sigma > 0$ are the asymptotic normalization parameters. They are called the location and the scale parameter, respectively. To be more precise, the location parameter specifies the center of the distribution, and the scale parameter determines the size of deviations about the location parameter.

[8] The return level $z(T)$ is defined as a value which, on average, is exceeded once in T years. This is obtained by inverting equation (4):

$$z(T) = \mu - \frac{\sigma}{\gamma}\left\{1 - \left[-\log\left(1 - \frac{1}{T}\right)\right]^{-\gamma}\right\}. \tag{5}$$

T is usually referred to as the return time.

[9] In case $\gamma \neq 0$, the log likelihood function for a sample $Z_1, \ldots, Z_n$ of iid GEV random variables is

$$l(\psi) = -n \log \sigma - \sum_{i=1}^{n}\left(1 + \gamma \frac{Z_i - \mu}{\sigma}\right)^{-1/\gamma}$$
$$- \left(1 + \frac{1}{\gamma}\right)\sum_{i=1}^{n}\log\left(1 + \gamma \frac{Z_i - \mu}{\sigma}\right), \tag{6}$$

where $\psi = (\mu, \sigma, \gamma)$, and provided that $1 + \gamma \frac{Z_i - \mu}{\sigma} > 0$, for $i = 1, \ldots, n$. The maximum likelihood estimator (MLE) $\hat{\psi}$ for ψ is obtained by maximizing equation (6). A great benefit of MLE is that it has several interesting and useful properties that lead to standard errors and confidence intervals. The main result is that MLE is unbiased and asymptotically normally distributed under the regularity condition $\gamma > -0.5$ [*Smith*, 1985]. The case $\gamma \le -0.5$ corresponds to very light tailed distributions, but this situation is rarely seen in practical applications.

2.2. Spatial GEV Model

[10] Let $Z(x)$ denote the total precipitation for a given period of time d, and at location x (expressed in longitude/latitude, or other geographic coordinates). Hereafter, call d the aggregation level or rainfall duration. The goal is to provide inference for the probability $P\{Z(x) < z\}$ for all locations x within a certain region (in our case Belgium). The spatial GEV model is defined as $Z(x) \sim GEV[\mu(x), \sigma(x), \gamma(x)]$, where the parameters characterizes the extreme precipitation and are possibly related to climatological and orographic effects. Let the response Z_{ij} be the annual maxima at site i $\{1, \ldots, n_s\}$ in year $j \in \{1, \ldots, n_i\}$, and x_i being the

coordinate of the ith site. If the responses are independent, the log likelihood of the spatial stationary GEV model is

$$l(\psi) = -\sum_{i=1}^{n_s} \sum_{j=1}^{n_i} \left[\log \sigma(x_i) + \left(1 + \gamma(x_i) \frac{Z_{ij} - \mu(x_i)}{\sigma(x_i)}\right)^{-1/\gamma(x_i)} \right.$$
$$\left. + \left(1 + \frac{1}{\gamma(x_i)}\right) \log \left(\frac{Z_{ij} - \mu(x_i)}{\sigma(x_i)}\right) \right], \tag{7}$$

where ψ is a vector of parameters that relates the GEV parameters $\mu(x)$, $\sigma(x)$, $\gamma(x)$ to the covariates. Regularity conditions for standard asymptotic likelihood results are not known for spatial GEV models. Just like in the single-site case, one assumes that violation of regularity conditions is rarely encountered in environmental modeling, albeit one has to be aware of this potential problem.

[11] For clarification some examples are provided that will be examined later in this study. Denote by $H(x)$ the altitude of location x, and propose the following three nested models $\text{GEV}_0 \subset \text{GEV}_{10}^{(alt)} \subset \text{GEV}_{11}^{(alt)}$:

[12] 1. GEV_0 defined by $\psi = (\mu_0, \sigma_0, \gamma_0)$ is the classical model with all parameters being constant:

$$\mu(x) = \mu_0, \qquad \sigma(x) = \sigma_0, \qquad \gamma(x) = \gamma_0. \tag{8}$$

[13] 2. $\text{GEV}_{10}^{(alt)}$ defined by $\psi = (\mu_0, \sigma_0, \gamma_0, \mu_1)$ is the model with location parameter linearly dependent on the altitude:

$$\mu(x) = \mu_0 + \mu_1 H(x), \qquad \sigma(x) = \sigma_0, \qquad \gamma(x) = \gamma_0. \tag{9}$$

[14] 3. $\text{GEV}_{11}^{(alt)}$ defined by $\psi = (\mu_0, \sigma_0, \gamma_0, \mu_1, \sigma_1)$ is the model with location and scale parameters linearly dependent on the altitude:

$$\mu(x) = \mu_0 + \mu_1 H(x), \qquad \sigma(x) = \sigma_0 + \sigma_1 H(x), \qquad \gamma(x) = \gamma_0. \tag{10}$$

[15] In environmental sciences, there are numerous papers devoted to the inclusion of covariates in parameters of extreme value distributions. Most of them are concerned with modeling nonstationarity or temporal dependence, and use covariates such as time, indices of large-scale atmospheric processes or seasonal effects [*Smith*, 1989; *Coles*, 2001; *Katz et al.*, 2002; *El Adlouni et al.*, 2007].

2.3. Adjusting for Spatial Dependence

2.3.1. Error Estimation

[16] Maximum likelihood estimation is based on the assumption of independence among series. The asymptotic properties of the independence MLE are well known, but however, this is not the true model, especially when the station network is dense. A solution to account for the dependence is ignoring the dependence initially, thus working with MLE under misspecification, and then making adjustments to estimates of parameter uncertainty [*Davison*, 2003; R. L. Smith, unpublished manuscript, 1990b]. More precisely, one has

$$\hat{\psi} \to N\left(\psi_0, I(\psi_0)^{-1} V(\psi_0) I(\psi_0)^{-1}\right), \qquad \text{as } m \to \infty, \tag{11}$$

where ψ_0 is the vector of true parameters, $V(\psi_0) = \text{cov}[\nabla l(\psi_0)]$, and $I(\psi_0)$ the Fisher information matrix. If the assumed model was correct (i.e., the series are independent), one would have $I = V$ and the classical approximation is recovered.

[17] Suppose that the series contributing to $l(\psi)$ are not independent, but the contributions h_i from the separate years are. Writing $\nabla l(\psi) = \Sigma_i \nabla h_i(\psi)$ expresses as a sum of n independent terms. Then one gets (R. L. Smith, unpublished manuscript, 1990b)

$$V(\psi_0) = n \, \text{cov}[\nabla h_i(\psi_0)], \tag{12}$$

which can be approximated using the empirical covariance matrix of the observed $\nabla h_i(\hat{\psi})$.

2.3.2. Model Selection

[18] Having two different models in mind, one wants to know which one should be preferred for modeling our data. If two models have the same maximized log likelihoods, one should prefer the one with fewer parameters because it will have a smaller variance. However, if only a small increase in maximized log likelihoods is found, it remains to be seen whether this small increase is worth the price of having additional parameters, and hence a larger variance. A commonly used test statistic is the Akaike information criterion (AIC). However, when working with spatial correlated data, the AIC is not appropriate. An extension of the AIC that accounts for misspecification is the Takeuchi Information Criterion (TIC), defined as

$$\text{TIC} = -2l(\hat{\psi}) + 2\text{Tr}\left[I(\hat{\psi})^{-1} V(\hat{\psi})\right], \tag{13}$$

where $l(\hat{\psi})$ is the approximate likelihood from equation (7), $I(\hat{\psi})$ and $V(\hat{\psi})$ are as before. It was recently rederived by *Varin and Vidoni* [2005]. The best model will be that having the lowest value of TIC. If the assumed model was correct, the classical AIC is recovered.

3. Precipitation Data

[19] Two different networks covering the Belgian territory are currently available, the climatological and hydrometeorological network. The former is based on daily measurements of temperature, precipitation, pressure, etc.; while the second is aimed at evaluating precipitation, temperature and humidity at a much higher rate (every 10 min) in order to compute quantities relevant for hydrological modeling like fast runoffs. Measurements provided by both networks have been extensively used for climatological analysis [*Sneyers*, 1960, 1975; *Sneyers et al.*, 1989; *Demarée*, 1985; *Dupriez and Demarée*, 1988, 1989; *Gellens*, 1995, 2000, 2002, 2003; *Delbeke*, 2001; *Willems*, 2000; *Vannitsem and Naveau*, 2007; *Ntegeka and Willems*, 2008].

[20] In our study, k-daily precipitation is obtained by aggregation of daily measurements of the climatological network. Total precipitation amounts over a period shorter than (or equal to) 24 h are obtained by aggregation of 10 min data of the hydrometeorological network.

3.1. The Climatological Network

[21] The climatological network started to operate in 1833. At that time it was based on a few key stations, and it is nowadays composed with more than 650 stations. During its long existence, this network has experienced several
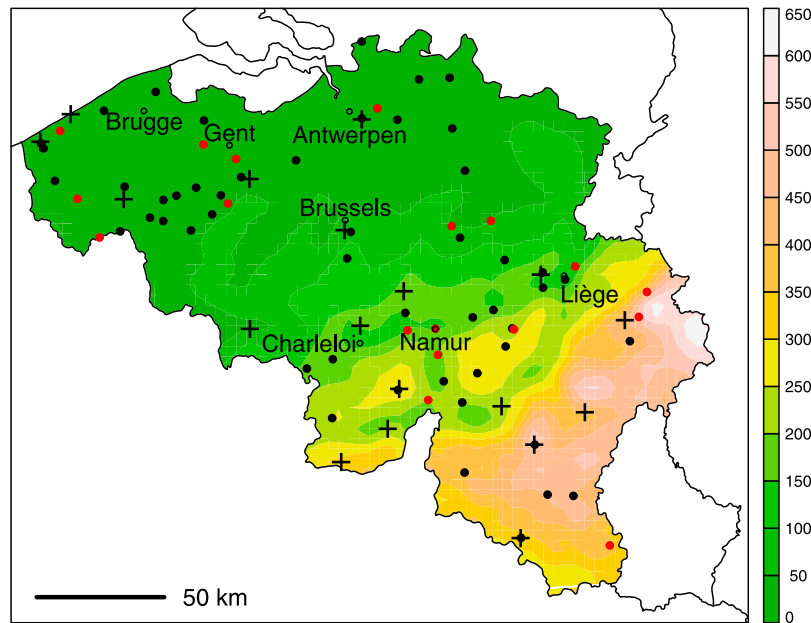
Figure 1. Elevation map (m) of Belgium, together with the location of the climatological stations (black dots, calibration stations; red dots, validation stations) and hydrometeorological (crosses) stations.

changes such as displacements and withdrawals of stations. To work with an homogeneous network, a subset of stations has been selected covering a common period from 1951 up to present without substantial interruptions.

3.2. The Hydrometeorological Network

[22] A Hellmann-Fuess pluviograph was installed at the climatological station of the Royal Meteorological Institute of Belgium at Uccle in 1898, and is continued to date [*Demarée*, 2003]. The series is recorded by the same instrument at the same location since 1898 and processed with identical quality since that time. The measuring frequency is unique as well: 10 min with more than 110 years of continuous data. In 1968, 18 additional pluviographs were installed, providing a spatial coverage of the country for hydrological purposes. This network is less dense than the climatological one and some stations display long periods with missing data. These series ended at 2005, and the pluviographs are nowadays progressively replaced by automatic stations. The latter measurements are not included in the study.

3.3. Homogeneity Testing

[23] It is often important to determine if a set of data is homogeneous before any statistical technique is applied to it. Homogeneous data are drawn from a single population. In other words, all outside processes that could potentially affect the data must remain constant. Inhomogeneities in station data records are often caused by changes in observational routines, among which are station relocations, changes in measuring techniques and changes in observing practices. Without assurance of homogeneity, parameter estimates will be unreliable. For this reason, the series are statistically tested with respect to homogeneity. The two-step approach of *Wijngaard et al.* [2003] includes, first, four homogeneity tests, and secondly, on the basis of these tests

the series are grouped in an overall classification of reliability: "useful," "doubtful" and "suspect." All the series of the climatological network that contain 60 years of (more or less) continuous data have been examined and 68 series were assigned to the class "useful." Likewise, the series of the hydrometeorological network has been tested and 18 stations are selected. Series containing some missing years were also considered in our study, simply because 10 min measurements are quite limited. Figure 1 shows the location of the stations selected. Among the 68 stations of the climatological network, 18 are excluded from the analysis for validation, and thus 50 are used for inference. For reasons of scarcity of 10 min series, the 18 stations of the hydrometeorological network are used for validation and inference as well.

[24] Besides anthropogenic influences also homogeneity with respect to climate change needs to be assumed and tested for. The Mann test which provides information on the presence of tendencies, has already been applied to the climatological network [*Gellens*, 2000; *Vannitsem and Naveau*, 2007]. Their analysis reveals that the vast majority of the time series recorded for summer are stationary. For winter, the results are different: about 2/3 of the stations are nonstationary at the 5% level. For operational purposes, statistical practitioners use stationary models notwithstanding that climatic series are known to be nonstationary. Of course, one can criticize that, but one should take in mind that there is simply no alternative.

4. Spatial Variation of GEV Parameters

[25] In this section, the regional variability in the GEV parameters is tested. Denote one of the classical GEV parameters by φ. Let φ_i be the parameter at the ith site, $\hat{\varphi}_i$ its MLE. Under the assumption that annual maxima are spatially independent, the null hypothesis $\varphi_1 = \varphi_2 = \ldots = \varphi_{n_s} \equiv$

Table 1. Values of X^2 Statistic in Equation (14) for Testing Regional Differences in the GEV Parameters[a]

	d (min)				
	10	20	30	60	120
μ	52.4	51.4	37.1	29.9	31.0
σ	26.9	25.5	28.3	31.2	27.0
γ	22.0	8.8	14.9	16.2	14.7

[a]Recall that $P\{\chi^2_{17} \leq 27.59\} = 0.95$.

φ can be tested with the statistic [*Buishand et al.*, 2009; *Overeem et al.*, 2008]

$$X^2 = \sum_{i=1}^{n_s} (\hat{\varphi}_i - \bar{\varphi}_w)^2 / \sigma^2(\varphi_i), \qquad (14)$$

with $\bar{\varphi}_w$ the weighted average of the $\bar{\varphi}_i$'s, relative to the record length, and $\sigma^2(\varphi_i)$ the variance of MLE. Spatial dependency of annual maxima of the 18 hydrometeorological stations can be neglected for short durations. Cross correlations become apparent from $d = 6$ h. Next, X^2 was calculated for $d = 10, 20, 30, 60$ and 120 min. Under the null hypothesis, the statistic X^2 has a χ^2 distribution with $n_s - 1$ degrees of freedom. From Table 1 it can be seen that there is a strong evidence for regional variability in the location parameter μ. In contrast, the shape parameter γ is likely to be constant over the different sites since X^2 values are far below the 5% critical value. It was difficult to conclude the variability in the scale parameter σ with high confidence because X^2 is fluctuating around this critical value.

[26] For larger durations, a technical difficulty with testing for regional differences in the GEV parameters is that the estimates are spatially correlated due to the spatial correlation of annual rainfall maxima. In the presence of spatial dependence, the statistic in equation (14) can be extended to [*Witter*, 1984]

$$X^2 = (\hat{\boldsymbol{\varphi}} - \bar{\varphi}_w \mathbf{e})^T \mathbf{C}^{-1} (\hat{\boldsymbol{\varphi}} - \bar{\varphi}_w \mathbf{e}), \qquad (15)$$

with $\bar{\varphi}_w$ the generalized least squares estimate of φ

$$\bar{\varphi}_w = \frac{\mathbf{e}^T \mathbf{C}^{-1} \hat{\boldsymbol{\varphi}}}{\mathbf{e}^T \mathbf{C}^{-1} \mathbf{e}}, \qquad (16)$$

where $\mathbf{C}$ is the covariance matrix of $\hat{\boldsymbol{\varphi}} = (\hat{\varphi}_1, \ldots, \hat{\varphi}_{n_s})^T$, and $\mathbf{e}$ is a vector with n_s ones. Under the null hypothesis one has $X^2 \sim \chi^2_{n_s-1}$. The elements of $\mathbf{C}$ are obtained with a bootstrapping procedure that accounts for spatial correlation. A bootstrap sample is constructed by resampling years 1951–2010 with replacement and thus consists of 60 years times 68 annual maxima. Remark that spatial correlations are not preserved if annual maxima series were resampled from each individual station. From each bootstrap φ_i ($i = 1, \ldots, n_s$) is reestimated by MLE. Spatial correlations between $\hat{\varphi}_i$ and $\hat{\varphi}_j$ are then estimated from 10^4 bootstrap samples. Only k-daily extremes were considered here since the number of 10 min series (i.e., 18) is clearly too low, and their length is too short for the present analysis. From 68 stations one can form 4556 pairs for which the correlation coefficient can be computed. These estimations exhibit large variability as can be seen from Figures 2 and 3 for $d = 1$ day and 10 days. However, when testing for regional differences with equation (15), it is

not allowed to introduce such highly variable estimations in $\mathbf{C}$. Indeed, the use of the χ^2 distribution in the test assumes that $\mathbf{C}$ is known in advance; $\mathbf{C}$ can be possibly replaced by an estimated covariance matrix provided that the estimation
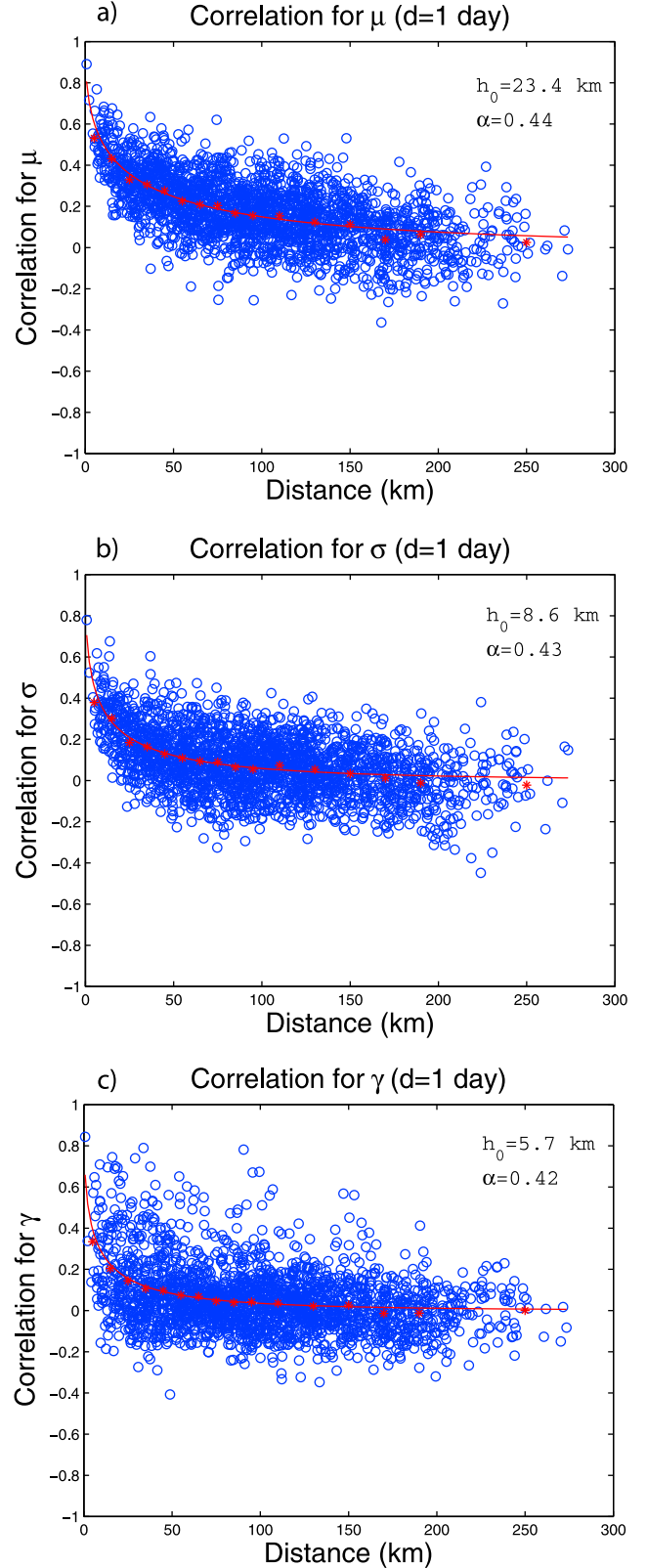
Figure 2. Correlation between GEV parameters as a function of the distance for $d = 1$ day.
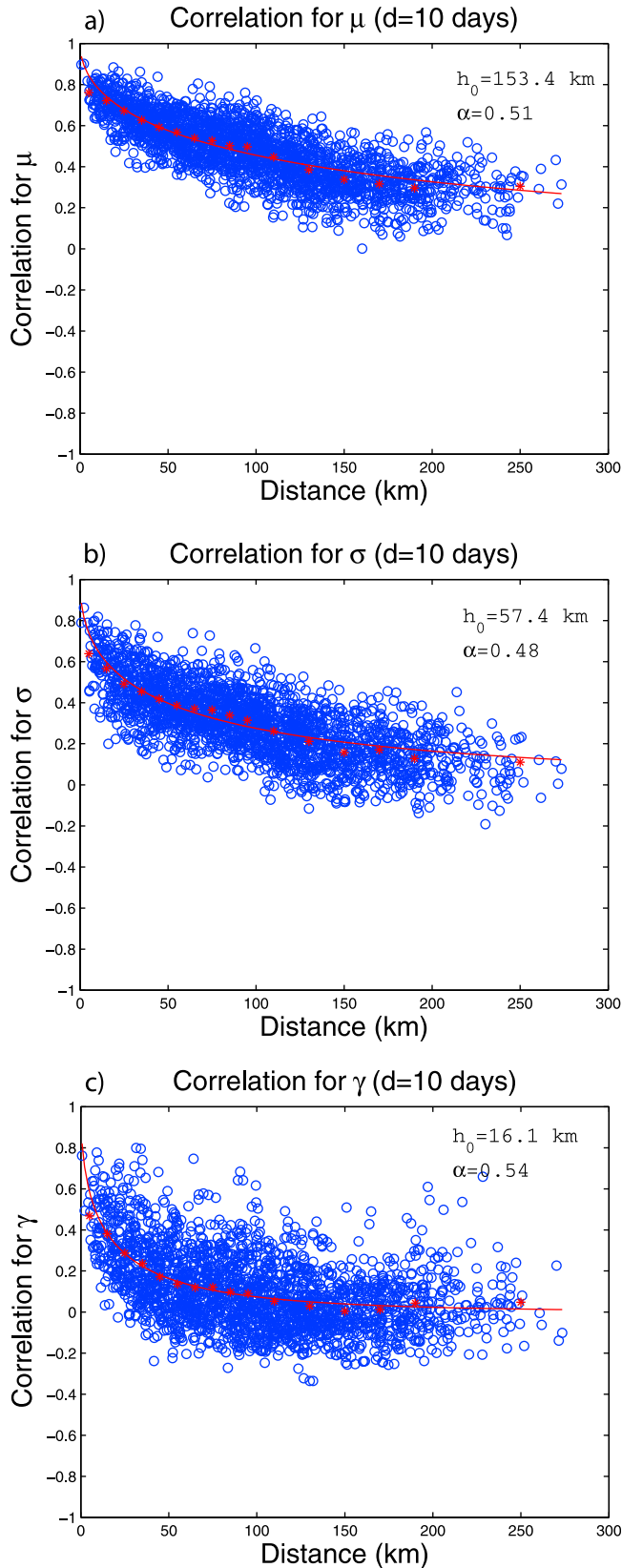
Figure 3. Correlation between GEV parameters as a function of the distance for $d = 10$ days.

variance is small. This is obtained by fitting a suitable model to the computed correlations. The following exponential model is commonly used [*Buishand et al.*, 2009; *Overeem et al.*, 2009]

$$\rho(h) = \exp\left[-\left(\frac{h}{h_0}\right)^{\alpha}\right], \qquad (17)$$

where $\rho(h)$ is the correlation at the intersite distance h (km), h_0 (km) a scale parameter and α a shape parameter. The parameters α and h_0 are estimated based on the modified least squares method that is fully described by *Buishand et al.* [2009, Appendix 3]. The model gives a reasonable description of the decay of ρ with intersite distance, as can be seen in Figures 2 and 3. Here is $\alpha < 1$, which means that the correlation decays slower than the exponential function. For $h = h_0$, one has $\rho = e^{-1} \approx 0.37$. According to Belgian studies included by *Gellens* [2000] and *Vannitsem and Naveau* [2007], there is an increasing dependency for growing aggregation levels. Short-duration rainfall extremes are usually associated with convective thunderstorm activities. On the other hand, long-duration extremes can be linked with large-scale atmospheric situations and thus exhibit higher intersite correlations over long distances, which is confirmed by the larger values of h_0 in Figure 3 compared to Figure 2.

[27] Now, the covariances in **C** can be calculated by multiplying the variance on the main diagonal with the modeled correlation coefficient in equation (17). The resulting X^2 values, listed in Table 2, indicate that there is a strong evidence for spatial differences in the location parameter μ. Also the scale parameter σ is subject to spatial differences, but it is less significant. Finally, variations in the shape parameter γ are not statistically significant, and will be kept constant in our modeling approach (section 5).

5. Modeling of Extreme Rainfall

5.1. Study Region and Selection of Covariates

[28] Roughly speaking, the study area has two different subregions. In the north part of Belgium there are plains which belong to the coastal region of the North Sea. The southern section is formed by the plateau of the Ardennes where mountain heights range from 400 to almost 610 m. To produce return level maps, one has to specify GEV models over continuous space, as explained in section 2.2. The foregoing study suggests to model spatial variability through the location and scale parameters, i.e., $\mu(x)$ and $\sigma(x)$, and keeping the shape parameter constant, $\gamma(x) = \gamma$. The first question to be answered is which are the best possible choices for the covariates. Geographically coordinates (longitude, latitude, altitude) are readily available in the form of

Table 2. Values of X^2 Statistic in Equation (15) for Testing Regional Differences in the GEV Parameters[a]

					d (days)						
	1	2	3	4	5	7	10	15	20	25	30
μ	256	342	398	447	503	663	703	838	869	1071	1201
σ	95	93	129	108	134	133	126	139	124	115	110
γ	69	63	61	67	73	70	70	45	62	65	76

[a]Recall that $P\{\chi^2_{67} \leq 87.11\} = 0.95$.
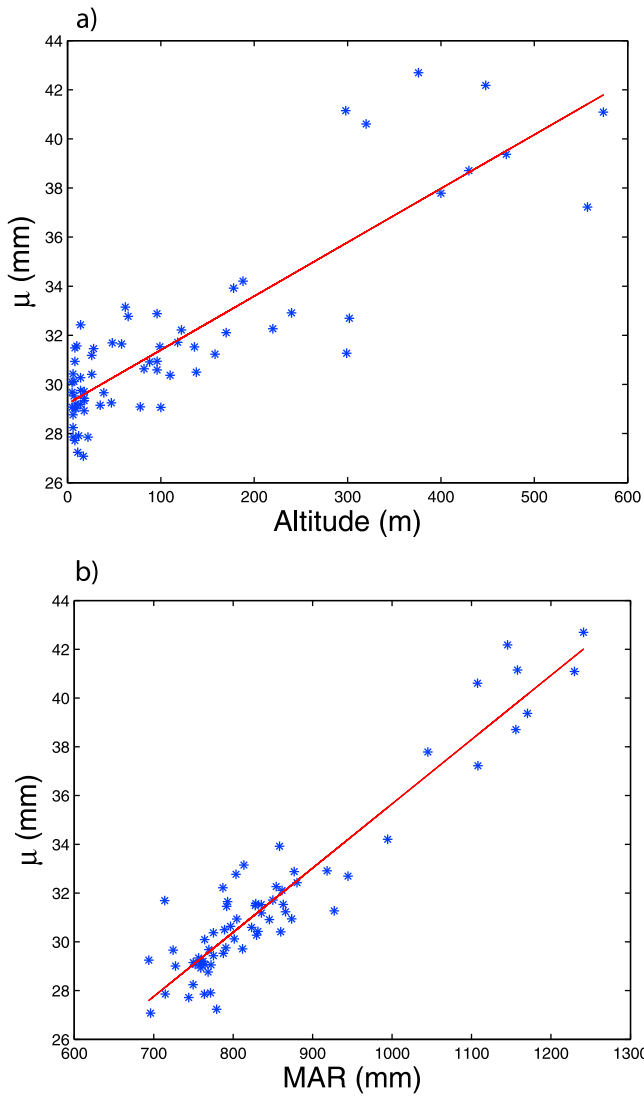
Figure 4. Scatterplot of μ (daily rainfall) for every station against the altitude and mean annual rainfall (MAR).

digital terrain models, and are commonly used in spatial regression studies [*Blanchet and Lehning*, 2010; *Cooley et al.*, 2007; *Northrop and Jonathan*, 2011]. In addition, distance from the sea is also a useful covariate to assist the mapping of extreme rainfall [*Faulkner and Prudhomme*, 2007]. Beside, there are several other possibilities proposed in the literature. For example, *Weisse and Bois* [2001] have explained the characteristics of heavy rains in the French Alps by detailed topographic characterization of relief in order to map rainfall risks. The above mentioned variables are known as geographical covariates. Another important class consists of climatological covariates which link the regional variability of extremes with climatological patterns [*Blanchet and Lehning*, 2010; *Cooley et al.*, 2007]. The scatterplots in Figure 4 indicate that for the location parameter the mean annual rainfall (MAR) is even more informative than elevation. In a comparative study, the following covariates are considered in the location parameter: (1) longitude/latitude, (2) distance to the sea, (3) elevation and (4) MAR. Analogous to elevation-dependent models (i.e., equations (8)–(10)), one can introduce nested models

linearly depending on one of these covariates. In Figure 5, model quality has been assessed by using TIC as a guide. Here, models with covariates for μ (i.e., GEV_{10}) were considered. As expected, adding covariates to μ greatly decreases TIC values, and the differences become larger for growing aggregation levels. For durations smaller than 6 h, TIC differences are less pronounced. In any case, it turns out that MAR and elevation are the best choices, and furthermore, MAR outperforms the elevation as a covariate. It is difficult to discern much of the spatial signal in the traditional longitude/latitude space or distance to the sea, so that maps produced by these models inadequately describe extreme precipitation.

5.2. Parameter Inference

[29] Here, GEV models with covariates including elevation and MAR are investigated in greater detail. Denote by $GEV_0 \subset GEV_{10}^{(mar)} \subset GEV_{11}^{(mar)}$ the nested models linearly depending on MAR. The maximization of the likelihood $l(\psi)$ in equation (7) was done using the MATLAB optimization
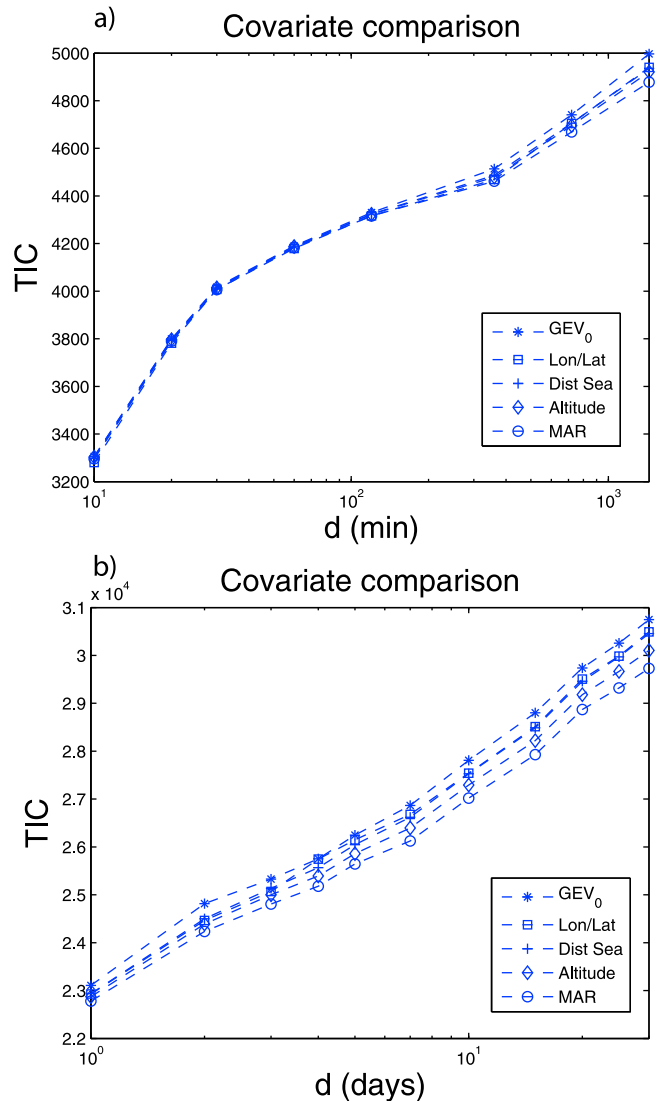
Figure 5. TIC against rainfall duration. Covariates for location parameter. (a) Short durations 10–1440 min. (b) Long durations 1–30 days.
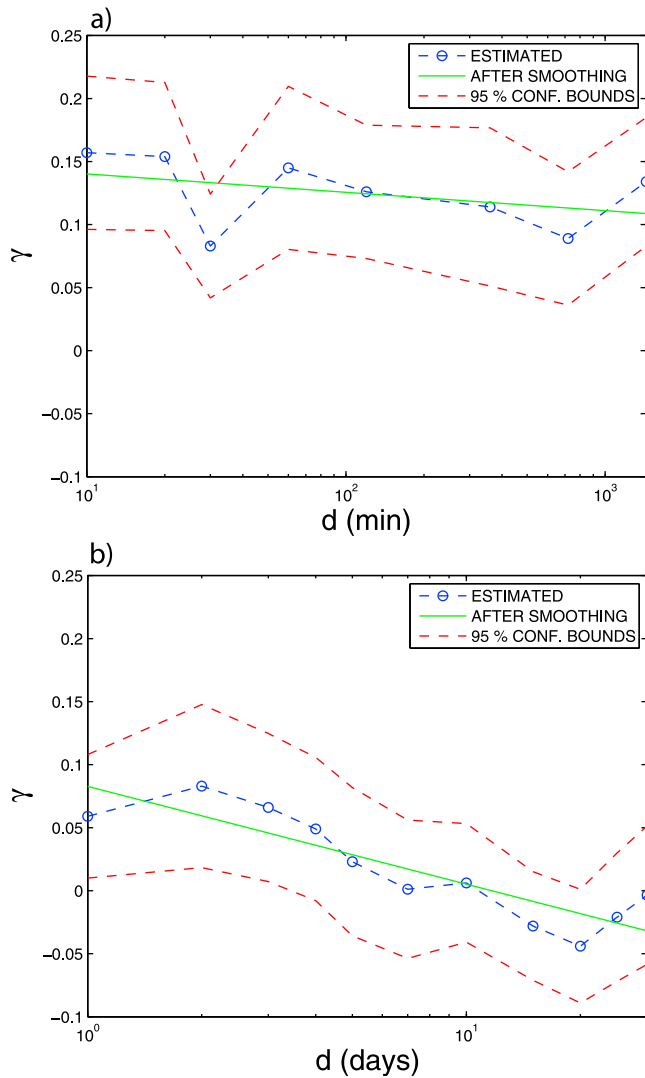
Figure 6. Estimation of shape parameter γ against the aggregation level d. Model $GEV_{11}^{(alt)}$.

algorithm fminunc. This procedure starts at an initial value and attempts to find a local minimum of $-l(\psi)$. Thousand initial start values are randomly generated, and the estimate $\hat{\psi}$ with the smallest local minimum was finally kept. By using TIC, it was found that GEV_{11} models are the most optimal ones. Estimation results of γ from $GEV_{11}^{(alt)}$ against the aggregation level d are shown in Figure 6. In addition, 95% confidence intervals are also plotted. The estimation results of location and scale parameters are yet not shown, but first need to be slightly modified, for reasons that will be explained here. For all the models it was found that $\mu(d_1) <$

$\mu(d_2)$ and $\sigma(d_1) < \sigma(d_2)$ for two different duration times $d_1 < d_2$. Under this circumstance it is absolutely necessary that $\gamma(d_1) \geq \gamma(d_2)$. This is easily seen when plotting the return level $z(T)$ against T. If one had $\gamma(d_1) < \gamma(d_2)$, then the graphs of $z_1(T)$ of $z_2(T)$ should intersect each other at some T, which is physically impossible. Observing Figure 6, estimations of γ are inconsistent at several places. For example, in Figure 6b (k-daily precipitation), the highest value of $\hat{\gamma}$ is reached at 2 days instead of 1 day. To guarantee consistency, the estimations are smoothed by fitting the curve

$$\gamma(d) = a - b\,ln(d) \qquad (18)$$

to the points $(d_i, \hat{\gamma}(d_i))$ [*Buishand*, 1983; *Buishand et al.*, 2009; *Gellens*, 2003]. The result of the curve fitting for the k-daily data are listed in Table 3. The use of these modeled γ values is justified because they are included in the 95% confidence intervals from the original raw estimations (see Figure 6). For low aggregation levels (Figure 6a), it can be seen that there is no remarkably variability in $\hat{\gamma}$, except for $d = 30$ min and 1440 min. Note that for short durations, some other regression relations, different from equation (18), are known in the literature. In a similar study for the Netherlands, one has simply put $\gamma = 0.09$ [*Buishand and Wijngaard*, 2007]. On the other hand, *Gellens* [2003] proposed a linear relationship between γ and d but anyhow, the mean value agrees very well with $\gamma = 0.09$. Despite the fact that the same data are used, our study reveals that the mean value equals 0.125, a difference that could be explained because the L moment estimator was used by *Gellens* [2003]. In order to be consequent select the same type of model as for daily data; fitting results are again listed in Table 3. Consistency between models for short and long durations can be observed from Figure 6 because equation (18) evaluated at $d = 1$ day (Figure 6b) is included in the 95% confidence interval of γ of 24 h extremes obtained from 10 min data (Figure 6a), and vice versa. The additional γ estimations for $GEV_{11}^{(mar)}$ in Table 3 show a fairly small difference with those of $GEV_{11}^{(alt)}$.

[30] Next, for each aggregation level the modeled γ value (see Table 3) is introduced in the log likelihood in equation (7), and the remaining parameters are reestimated. The complete output is recorded in Tables A1–A4 of Appendix A. Including covariates to σ yields a slightly lowering of the TIC values. Especially for short durations, the TIC values are barely changed. According to TIC, models with covariates in μ and σ have been selected for further investigation.

[31] Finally, by using these models 20 year precipitation return level maps for Belgium can be produced. In Figure 7, only short durations are considered since daily and two-daily extremes need to be adjusted (see section 6). The standard deviation of the error in the return levels is also plotted, which could be calculated by means of the well-known delta

Table 3. Fitting Results of Equation (18) to Raw Estimations of γ, Together With the Standard Error[a]

	$1 \leq d \leq 1440$ (d (min))		$1 \leq d \leq 30$ (d (days))	
	a	b	a	b
$GEV_{11}^{(alt)}$	0.15482 (0.02918)	0.00633 (0.00590)	0.08282 (0.01316)	0.03372 (0.00597)
$GEV_{11}^{(mar)}$	0.14619 (0.02921)	0.00489 (0.00590)	0.08870 (0.01673)	0.03715 (0.00759)

[a]Values in parentheses are the standard errors.
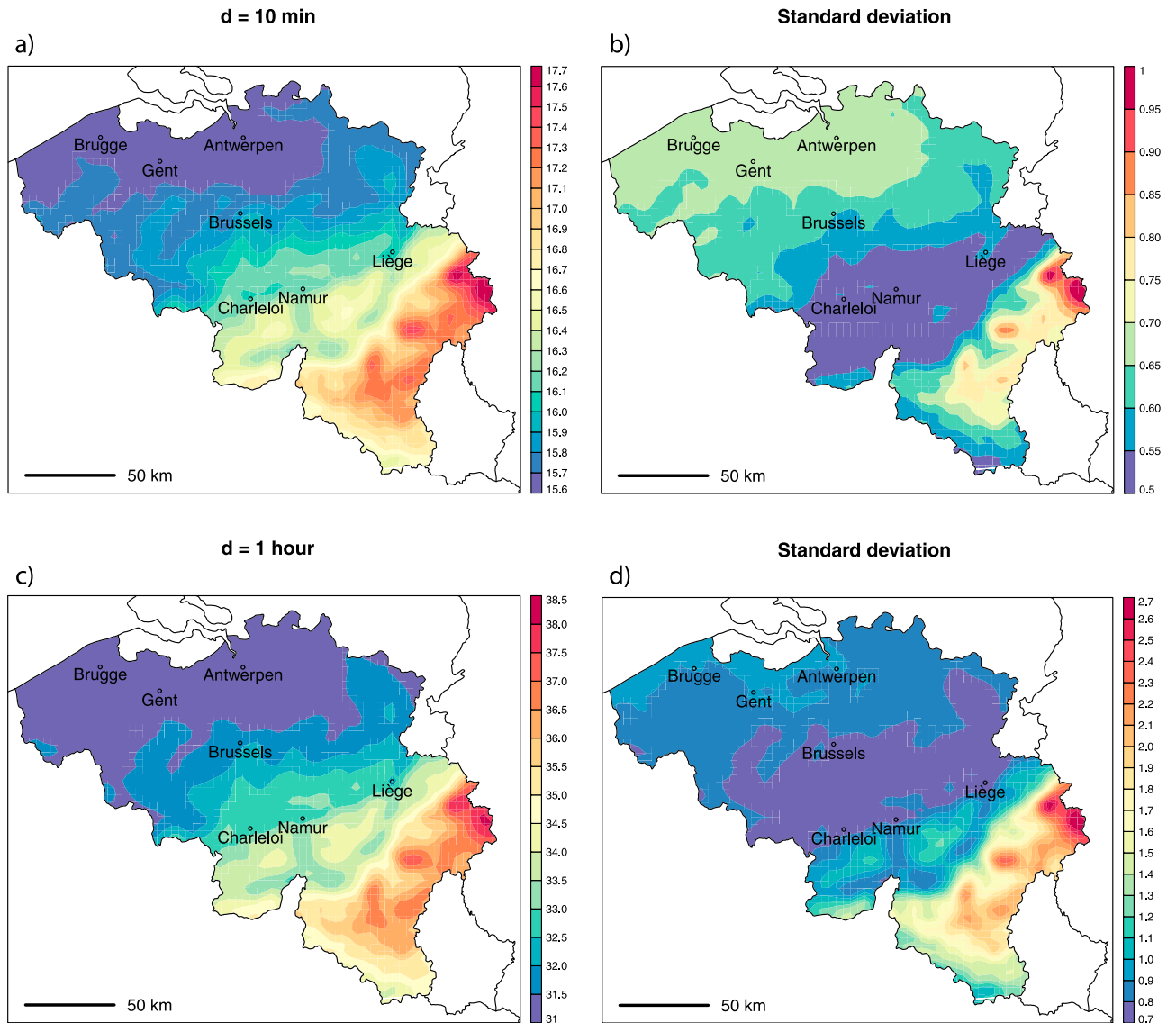
Figure 7. (left) Return level maps (mm) for return period $T = 20$ years. Model $\text{GEV}_{11}^{(alt)}$. (right) Corresponding standard deviation of the error (see equation (19)).

method [*Coles*, 2001]. In short, let $J_\psi \in \mathcal{R}^{n_p \times n_p}$ be the covariance matrix of $\hat{\psi}$, given by equation (11). Then the MLE of return level $z(T)$ has variance

$$J_z = \nabla z^t J_\psi \nabla z, \tag{19}$$

with

$$\nabla z = \left[\frac{\partial z}{\partial \psi_1}, \ldots, \frac{\partial z}{\partial \psi_{n_p}}\right]^t. \tag{20}$$

From Figure 7 one observes that the error is not necessarily larger in higher regions. Indeed, for model $G_{11}^{(alt)}$, equation (19) represents a quadratic form in H that reaches the minimum around $H = 200$ m.

5.3. Model Checking

[32] Having fitted a model to a data set, one should evaluate how well the method describes or explains the available data. When dealing with regression plots, the goodness of fit typically is visually assessed by inspection of various kinds of residual plots. Concerning the climatological network, recall that quality assessment of the models is based on a validation data set (18 in total) and is actually different to the inference data set.

5.3.1. QQ Plots

[33] In the present context, classical QQ plots are not useful as the spatial data are not identically distributed. A possible extension of the classical QQ plots consists in transforming the data to variables that satisfy the iid property [*Beirlant et al.*, 2004]. Assume $Z(x_i) \sim GEV[\mu(x_i), \sigma(x_i), \gamma]$, $i = 1, \ldots, m$. The transformation

$$R(x_i) = \frac{1}{\gamma} \log\left[1 + \gamma \frac{Z(x_i) - \mu(x_i)}{\sigma(x_i)}\right] \tag{21}$$

results in a Gumbel distributed random variable $R(x_i)$ [*Coles*, 2001; *Beirlant et al.*, 2004], i.e., $F[R(x_i) \leq r] = \exp[-\exp(-r)]$. The resulting Gumbel distribution does not
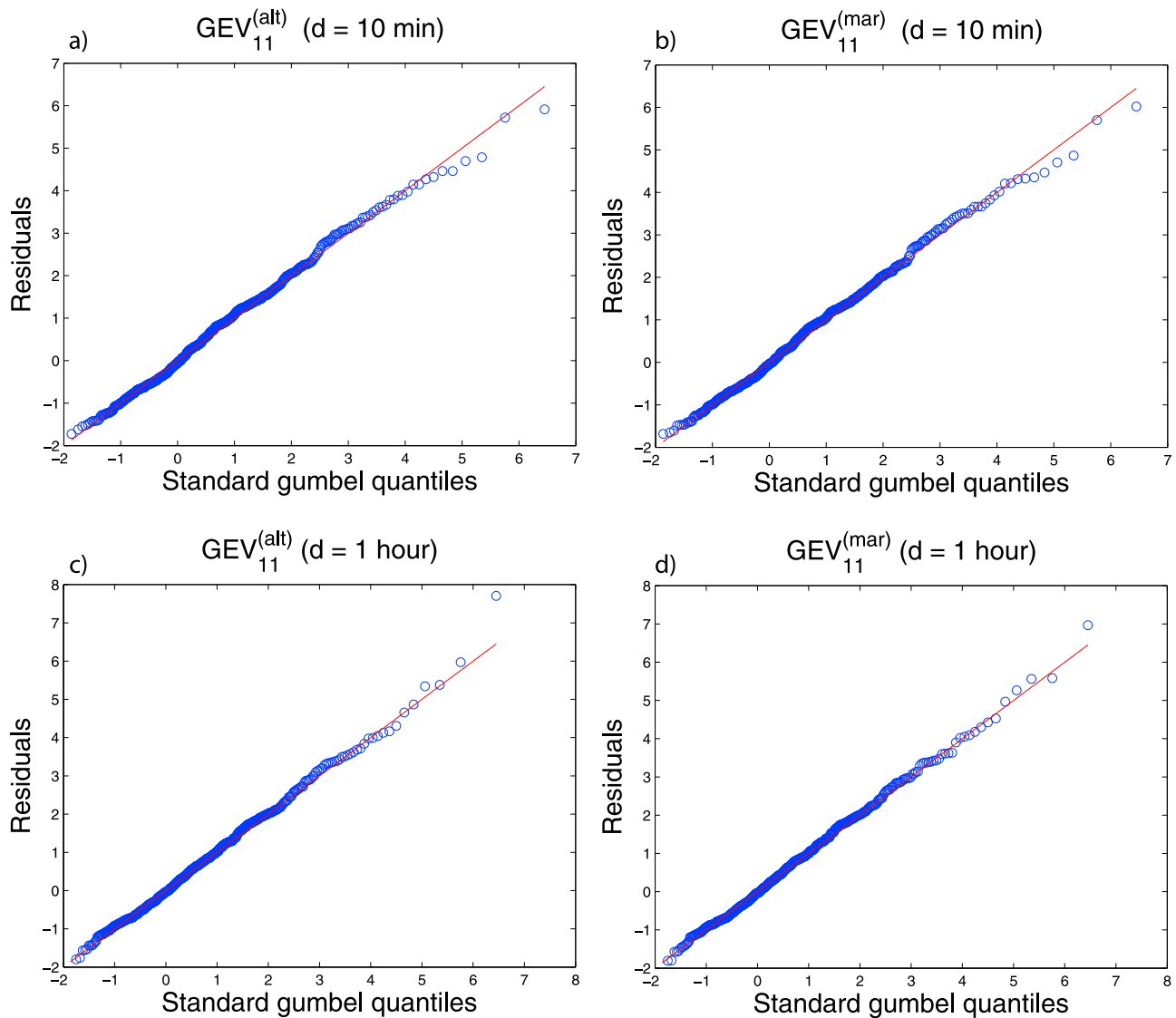
Figure 8. Data for short duration times ($d = 10$ min and $d = 1$ h): Gumbel QQ plot of the generalized residuals.

any longer depend on the covariates, and hence the random variable $R(x_i) =: R$ is identically distributed. Let n be the total number of annual maxima of the validation series. Define the corresponding order statistics by $R_{1,n} \leq \ldots \leq R_{n,n}$. The quantile function associated with the Gumbel distribution is given by

$$Q(p) = -\log(-\log p), \qquad 0 < p < 1, \qquad (22)$$

yielding the Gumbel QQ plot coordinates

$$\left(-\log\left(-\log \frac{i}{n+1} \right), R_{i,n} \right), \qquad i = 1, \ldots, n. \qquad (23)$$

The Gumbel model provides accurate description of the data, one expects the points on the Gumbel QQ plot to be close to the first diagonal.

[34] Figures 8 and 9 show Gumbel QQ plots for some aggregation levels. One can conclude that the GEV regression models describe the data quite well for lower aggregation levels. In such a case, Figures 8 and 9 indicate that there is hardly any difference between $\mathrm{GEV}_{11}^{(alt)}$ and $\mathrm{GEV}_{11}^{(mar)}$. It should be noted that the QQ plots for daily precipitation in Figure 9 could be misleading. At the first sight, one may conclude that the models are questionable because of the serious deviation to the first diagonal when $R > 3.1$. However, one should take into account that this includes only 4% of the available data, and the remaining points closely follow the first diagonal. Still, an excellent fit to the data is obtained. Differences between the two models become more apparent for higher aggregation levels. For $d = 10$ days, the QQ plot of $\mathrm{GEV}_{11}^{(alt)}$ possesses a systematic deviation when $R > 1$, which includes more that 30% of the data. In contrast, $\mathrm{GEV}_{11}^{(mar)}$ provides an excellent fit.

5.3.2. Hypothesis Testing

[35] At each station, the null hypothesis H_0 is proposed which states that the empirical distribution of annual maxima is consistent with the spatial GEV model. The null hypothesis is checked by two commonly used statistical tests: the Pearson's χ^2 test and the one-sample Kolmogorov-Smirnov test. A limitation of the hypothesis testing is that a rejection
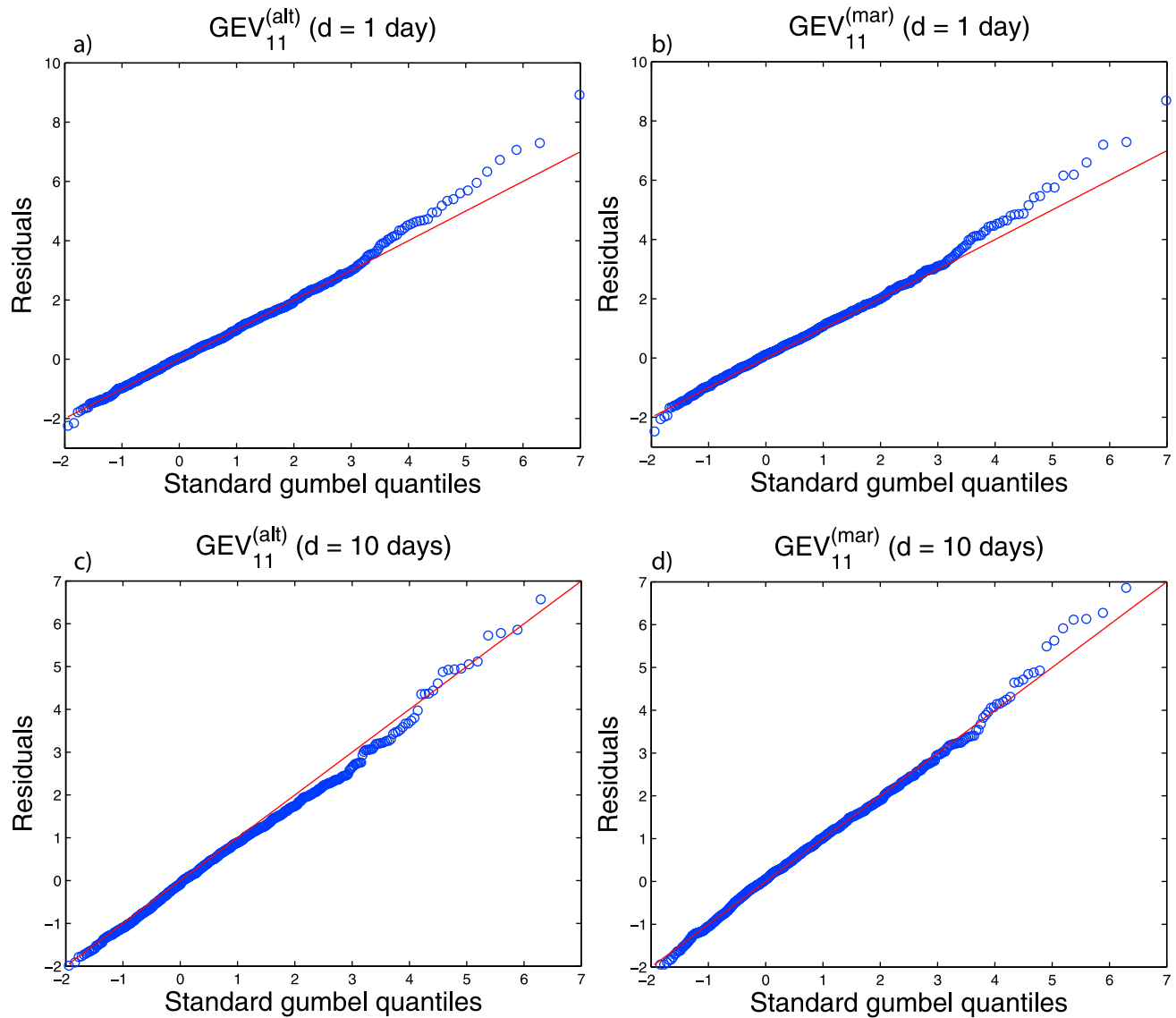
Figure 9. Data for long duration times ($d = 1$ and 10 days): Gumbel QQ plot of the generalized residuals.

at some location/duration can also be caused by an insufficiently good approximation to the GEV distribution by the validation data.

[36] The number of stations that have accepted H_0 at significance level 95% is listed for each duration in Tables 4 and 5, and serves as a kind of score of the model. One can conclude that the spatial GEV models describe the short duration extremes quite well. The overall performance of both models is quite similar, as expected. However, the

things change in case of longer aggregation levels, as can be seen from Table 5. Still, $GEV_{11}^{(alt)}$ performs acceptable for aggregation times up to 3 days, but from then, there is a decrease in model's performance.

6. Daily Versus 24 h Precipitation

[37] In practice, the GEV distribution of aggregated rainfall in time periods with fixed length and arbitrary starting

Table 4. Number of Series That Have Accepted H_0 at Significance Level 95%[a]

									d
	Test	10 m	20 m	30 m	1 h	2 h	6 h	12 h	24 h
$GEV_{11}^{(alt)}$	KS test	14	17	15	15	16	18	17	15
	χ^2 test	16	15	14	16	15	16	16	14
$GEV_{11}^{(mar)}$	KS test	14	17	16	16	17	18	18	17
	χ^2 test	16	16	14	15	15	17	18	16

[a]Pluviograph data, hydrometeorological network. In total, 18 stations are tested (see validation stations in Figure 1).

Table 5. Number of Series That Have Accepted H_0 at Significance Level 95%[a]

									d			
	Test	1	2	3	4	5	7	10	15	20	25	30
$GEV_{11}^{(alt)}$	KS test	17	16	14	12	12	12	12	12	12	12	14
	χ^2 test	16	17	15	15	11	13	13	12	13	14	14
$GEV_{11}^{(mar)}$	KS test	17	18	17	18	17	17	18	17	18	18	18
	χ^2 test	16	18	17	16	15	17	16	15	18	18	18

[a]Pluviometer data, climatological network. In total, 18 stations are tested (see validation stations in Figure 1).
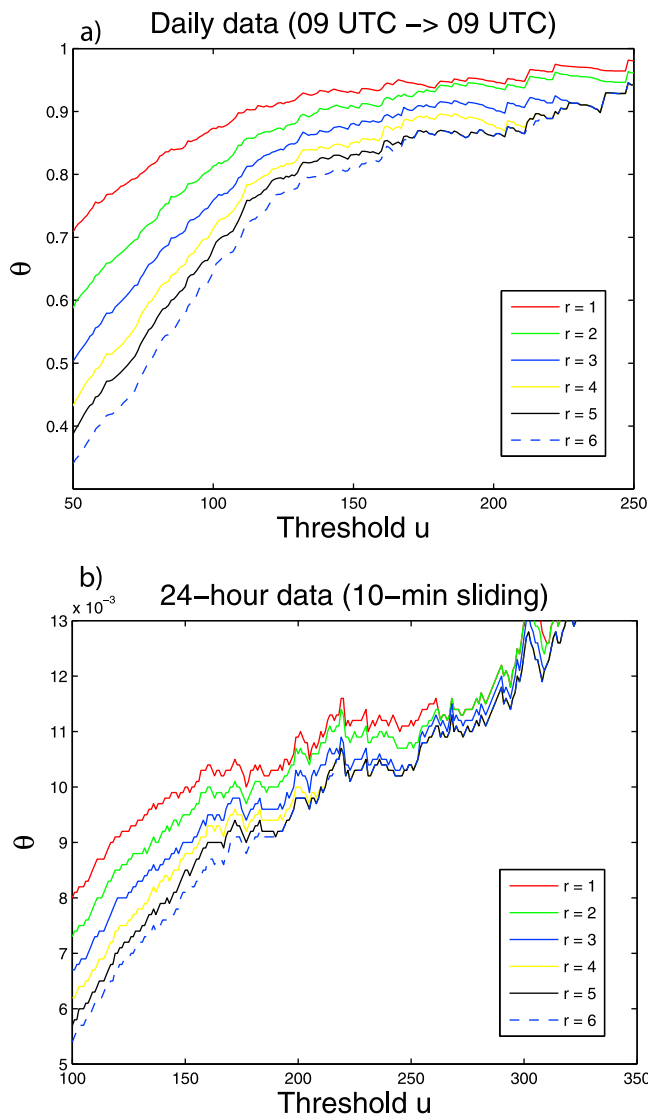
Figure 10. Estimation of the extremal index θ against threshold u for different r values.

points are often required, while in many cases data of observation days (09:00 UTC–09:00 UTC) are available. As said, the series of daily data is often longer, more reliable and the network of daily rain gauges is geographically denser. The question to be answered is if there is a link between the statistical properties of both types of extremes. Hydrologist have an empirical solution to this problem, using a scaling factor (the Hershfield factor) to relate the extremes of the two variables [see *van Montfort*, 1990, 1997].

[38] This issue will be placed in a more mathematical framework. If $X(t)$ is the rainfall intensity at time t, then $Y_i = \int_i^{i+24h} X(t)dt$ is the aggregated rainfall from time i over 24 h. The annual maxima of 24 h precipitation with arbitrary starting point, i.e., $\max_i\{Y_i\}$, are called sliding maxima. A good approximation of sliding maxima can be obtained with the maximum of 10 min sampled rainfall depths, the m block maxima being $M_m^{(24)} = \max\{Y_0, Y_{10}, \ldots, Y_{10(m-1)}\}$. Likewise, the annual maxima of daily observations are $M_m^{(D)} = \max\{Y_0, Y_{1440}, \ldots, Y_{1440[(m-1)/144]}\}$. Obviously, one has $M_m^{(D)} \leq M_m^{(24)}$. Denote by $G_{24}(x)$ and $G_D(x)$ the GEV distributions of

$M_m^{(24)}$ and $M_m^{(D)}$, respectively. A theoretical relation between the distributions $G_{24}(x)$ and $G_D(x)$, based on the extremal index has been proposed by *Robinson and Tawn* [2000]. However, in their work the sliding maxima are approximated by hourly sampling. A suitably adaptation of their relation to our case results in

$$G_{24}(x) = G_D^{\Theta}(x), \qquad \Theta = 144\,\theta_{24}/\theta_D, \qquad (24)$$

where θ_D and θ_{24} are the extremal indices of (1) daily data and (2) 24 h data, respectively, obtained by cumulating 10 min data. Straightforward calculations give [*Coles*, 2001]

$$\mu_{24} = \mu_D - \frac{\sigma_D}{\gamma}(1 - \Theta^\gamma), \qquad \sigma_{24} = \sigma_D\Theta^\gamma. \qquad (25)$$

More generally, one easily shows that the relationship between the annual extremes of k-daily precipitation (with sliding period of 24 h) and $24 \times k$-hourly precipitation can be obtained by replacing $D \to k\,D$ and $24 \to 24\,k$ in (24)–(25).

[39] The extremal index θ ($0 < \theta \leq 1$) is a quantity which, in an intuitive way, allows one to characterize the relationships between the dependence structure of the data and their extremal behavior. It plays an important role in extreme value analysis, with $\theta = 1$ indicating independence. Remark that θ is concerned with temporal dependence in one series, and not with spatial dependence between two series, see for example [*Buishand*, 1984]. Under some fairly mild condition (the so-called $D(u_n)$ condition of *Leadbetter et al.* [1983]), the extension of equation (2) to stationary sequences is

$$\Pr\{(M_n - b_n)/a_n \leq x\} \to G^\theta(x), \qquad \text{as } n \to \infty. \qquad (26)$$

The extremal index can be measured through the size of clusters of extreme values. A simple way of determining clusters of extremes is to define a sufficiently high threshold value u, and define consecutive exceedances of u to belong to the same cluster. The cluster is terminated when r consecutive values fall below u [*Coles*, 2001; *Beirlant et al.*, 2004]. The following estimator generally produces good estimates [*Robinson and Tawn*, 2000]

$$\hat{\theta} = \frac{n_c}{n_u}, \qquad (27)$$

where n_u is the number of exceedances of the threshold u, and n_c is the number of clusters above u. For other estimation methods, see *Beirlant et al.* [2004]. Careful choices of u and r are needed, as if r is too small, clusters can be dependent and if r is too large, n_c becomes too small.

[40] The foregoing theory has been applied to the more than 110 year time series of 10 min rainfall at Uccle (see section 3.2). First, it is instructive to make a sensitivity analysis for estimator (27). Figure 10 shows $\hat{\theta}$ against the threshold u for a variety of r values, $r = 1, \ldots, 6$. In Figure 10a, the estimations systematically increase until $u = 22.0$ mm, and hereafter they stay more or less stable. It is reasonable to choose u in this stable region. Figure 10 clearly shows that for these u values the estimations are not so sensitive to the selection of r values. Finally, one arrives at

$$\hat{\theta}_D = 0.95, \quad \hat{\theta}_{24} = 0.011, \quad \text{and thus} \quad \hat{\Theta} = 144\hat{\theta}_{24}/\hat{\theta}_D = 1.67. \qquad (28)$$

Table 6. Maximum Likelihood Estimation of the GEV Parameters for Annual Maxima of Daily Data (Sampled at 09:00 UTC) and 24 h Data, Obtained by Cumulating 10 min Data (Long-Term Uccle Series)[a]

$\hat{\mu}_D$	$\hat{\sigma}_D$	$\hat{\gamma}_D$	$\hat{\mu}_{24}$	$\hat{\sigma}_{24}$	$\hat{\gamma}_{24}$	$\hat{\mu}_{24}^*$	$\hat{\sigma}_{24}^*$
29.09 (0.87)	7.81 (0.67)	0.084 (0.090)	33.12 (0.87)	8.18 (0.65)	0.077 (0.069)	33.17	8.15
$\hat{\mu}_{2D}$	$\hat{\sigma}_{2D}$	$\hat{\gamma}_{2D}$	$\hat{\mu}_{48}$	$\hat{\sigma}_{48}$	$\hat{\gamma}_{48}$	$\hat{\mu}_{48}^*$	$\hat{\sigma}_{48}^*$
38.50 (0.99)	9.33 (0.73)	0.084 (0.064)	40.65 (0.99)	9.42 (0.72)	0.059 (0.060)	40.90	9.53

[a]The μ_{24}^* and σ_{24}^* are obtained with equation (25). Analogously for two-daily versus 48 h data.

As equation (27) shows that the extremal index is inversely proportional to the amount of extremal dependence, one has $\theta_{24} \ll \theta_D$ because there is much more serial dependence in the 10 min sampled 24 h series than in the daily series.

[41] The whole procedure has been repeated to the 10 min data of the hydrometeorological network (not shown). The estimations of Θ, which mutually differ slightly, have a mean value of 1.69 and is hardly different of the estimation (28) obtained from the long-term Uccle series.

[42] Next, when using the long-term Uccle series it can be examined how well the adjustment in equation (25) works in practice. Table 6 lists estimations of daily and two-daily extremes, together with the estimations of 24 and 48 hourly extremes which are based on (1) daily data (sampled at 09:00 UTC) and (2) direct estimation on aggregated 10 min data. Denote by μ_{24}^* and σ_{24}^* the estimations provided by equation (25). If one considers $\hat{\mu}_{24}$ and $\hat{\sigma}_{24}$ as the "true" parameters of $G_{24}(x)$, one may evaluate the quality of equation (25) with the "errors" $|\hat{\mu}_{24} - \mu_{24}^*|$ and $|\hat{\sigma}_{24} - \sigma_{24}^*|$. The results are promising for daily precipitation as the errors are around 0.02. For two-daily precipitation, the results are less good but are still largely acceptable, with errors in μ_{48} and σ_{48} of 0.25 and 0.11, respectively. It should be noted that μ_{48}^* and σ_{48}^* lie in the 95% confidence interval of μ_{48} and σ_{48}. Aggregation levels higher than 2 days are not considered since there is no strong evidence that μ_{3d} and μ_{72} seriously differ. Finally, return level maps of 24 h and 48 h precipitation are plotted in Figure 11. The calculation of standard errors slightly differs from section 5.2 and is obtained by substituting equation (25) into equation (19). Since Θ and model parameters ψ are not commonly estimated, the standard errors in Figure 11 cannot account for the uncertainty in Θ, so that one has to assume that $\hat{\Theta}$ presents the true value.

7. Conclusions

[43] The introduction of spatial GEV models is twofold. First, the idea of combining precipitation data at several sites in one single record, generally called regional frequency analysis, offers the possibility of getting reliable estimates of large quantiles. Second, the underlying parameters of the spatial GEV models are continuous in space, so that they can provide return levels at every place, even at stationless regions. The focus was on spatial differences (dependence on covariates) in the location and scale parameters of the GEV distribution. It was indeed shown that the shape parameter exhibits no significant spatial differences. However, one should take in mind that the present models are rather simple, and cannot completely explain the large variability in space. Think for instance of the impact of the urban heat island effect, or differences between precipitation in the coastal area and inland. Particularly, for durations smaller than 1 day there are only 18 series available, which may be insufficient to fully capture the regional differences. Anyway, the present methodology is still preferable than using estimations based on one single station for a whole region.

[44] The models presented in this study correspond to the cases in which the location and scale parameter are expressed as a linear relationship with a covariate. A comparative study has been made between models that are characterized by geographical or climatological covariates. It was difficult to discern much of a spatial signal in the traditional longitude/latitude space, and seems to inadequately describe extreme precipitation. Overall, it turned out that mean annual rainfall (MAR) is the strongest covariate for extreme precipitation. Beside, it is also likely that elevation has a significant influence on the climatological behavior of extreme precipitation. For short rainfall durations (less than 24 h), it was demonstrated that the performance of models including elevation or MAR are more or less equivalent. In conclusion, the effects not fully described by simple altitude-dependent relations are rather limited. However, serious discrepancies between both covariates arise for larger durations. In such case, models including elevation alone are not sufficient to explain data variance, and additional topographic aspects or relief characteristics should be taken into account.

[45] On the basis of foregoing tests, GEV models depending on MAR/elevation are selected for further research and practical purposes. Likelihood-based inference for extreme value models is based on the assumption that the series are independent. The methodology of R. L. Smith (unpublished manuscript, 1990b) ignores dependence, but adjusts inferences for dependence by modifying the estimation error (11). To avoid intersecting GEV distributions, a suitable function (18) was fitted to raw estimations of γ, and the remaining parameters were then reestimated. It should be noted that the fitted curves (18) lie within the 95% confidence bounds from the original estimations. The Takeuchi information criterion (TIC) was used to choose the most appropriate model. In any case, it was found that models with a covariate in the location and scale parameter are the most optimal ones. As expected, adding a covariate to the location parameter would substantially benefit model's performance. On the other hand, the effect of introducing a covariate in the scale parameter is rather limited, especially for short rainfall durations.

[46] It is tested if the spatial model is consistent with the empirical distribution of the individual validation sites with the commonly used Pearson's χ^2 test and the Kolmogorov-Smirnov test. The results of both tests are quite similar.
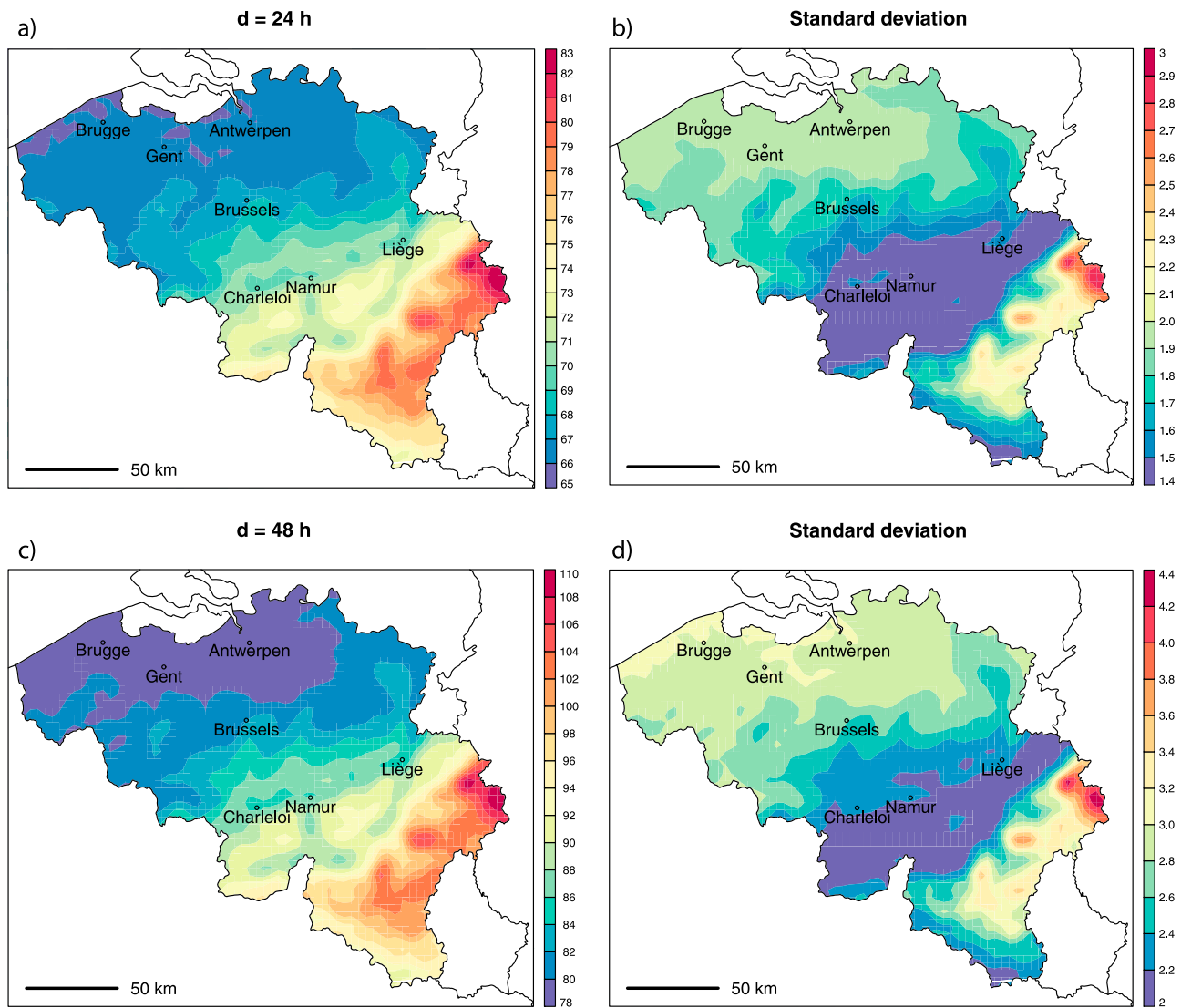
Figure 11. Return level maps (mm) of 24 h and 48 h precipitation, with return period $T = 20$ years. Model $\text{GEV}_{11}^{(alt)}$. Estimations are based on pluviometer data (climatological network), and then adjusted by equation (25).

Roughly speaking, for aggregation levels smaller than 3 or 4 days, both models explain a large part of the data variance, and are acceptable for operational purposes. The performance of altitude-dependent models is less satisfying for longer durations, but in contrast, MAR-dependent model are very promising. Furthermore, the QQ plots confirmed this statement. The validation is not concerned with a comparison of the model against the truth, which is unknown. Such a proper validation can be approached by simulation, as by R. L. Smith (unpublished manuscript, 1990b).

[47] Our models are finalized by accounting for the sampling frequency in daily (09:00 UTC–09:00 UTC) measurements. The transformation (25) of annual daily maxima to annual sliding 24 h maxima was specified accurately by estimating the extremal indices θ_D and θ_{24} from the more than 110 year time series of 10 min rainfall at Uccle. In addition, the estimations agree, on the average, very well with those obtained from the hydrometeorological observations.

Table A1. Estimation Results and Standard Errors for $\text{GEV}_{10}^{(alt)}$ [a]

d	$\hat{\mu}_0$ (mm)	$\hat{\mu}_1$ (mm/m)	$\hat{\sigma}$ (mm)	TIC
Pluviograph Data, Hydrometeorological Network				
10 m	6.59 (0.17)	6.65 e-4 (3.8 e-4)	2.60 (0.11)	3304.86
20 m	9.52 (0.24)	0.0011 (5.2 e-4)	3.83 (0.13)	3798.30
30 m	11.16 (0.27)	0.0014 (6.1 e-4)	4.70 (0.12)	4018.94
1 h	14.07 (0.34)	0.0014 (7.4 e-4)	5.21 (0.16)	4190.49
2 h	16.78 (0.38)	0.0032 (9.2 e-4)	5.89 (0.18)	4325.10
6 h	22.10 (0.55)	0.0090 (1.3 e-3)	6.73 (0.24)	4480.94
12 h	26.75 (0.69)	0.0128 (1.6 e-3)	8.10 (0.33)	4697.17
24 h	32.14 (0.83)	0.0197 (2.4 e-3)	9.63 (0.44)	4924.53
Pluviometer Data, Climatological Network				
1 day	29.05 (0.58)	0.019 (1.5 e-3)	9.08 (0.35)	22882.82
2 days	38.76 (0.81)	0.027 (2.4 e-3)	11.62 (0.54)	24407.67
3 days	45.14 (0.92)	0.033 (3.2 e-3)	13.01 (0.61)	25015.77
5 days	55.66 (1.25)	0.044 (3.6 e-3)	15.29 (0.64)	25869.67
7 days	64.06 (1.39)	0.054 (3.7 e-3)	16.88 (0.67)	26404.94
10 days	76.42 (1.58)	0.067 (4.7 e-3)	19.60 (0.77)	27303.60
15 days	92.41 (2.01)	0.085 (6.2 e-3)	23.19 (0.96)	28226.97
20 days	107.63 (2.43)	0.098 (6.8 e-3)	27.46 (1.29)	29188.31
30 days	134.40 (2.84)	0.127 (6.8 e-3)	31.98 (1.81)	30139.94

[a]The parameter γ is given in Table 3.

Table A2. Estimation Results and Standard Errors for $\text{GEV}_{11}^{(alt)\,a}$

d	$\hat{\mu}_0$ (mm)	$\hat{\mu}_1$ (mm/m)	$\hat{\sigma}_0$ (mm)	$\hat{\sigma}_1$ (mm/m)	TIC
		Pluviograph Data, Hydrometeorological Network			
10 m	6.50 (0.18)	0.0011 (4.7 e-4)	2.48 (0.15)	5.87 e-4 (4.6 e-4)	3302.50
20 m	9.36 (0.26)	0.0019 (6.8 e-4)	3.60 (0.19)	0.0011 (6.1 e-4)	3795.27
30 m	10.97 (0.29)	0.0024 (9.5 e-4)	4.37 (0.20)	0.0017 (9.3 e-4)	4015.16
1 h	13.77 (0.34)	0.0030 (1.3 e-3)	4.78 (0.20)	0.0023 (1.1 e-3)	4184.29
2 h	16.44 (0.40)	0.0051 (1.5 e-3)	5.34 (0.22)	0.0029 (1.2 e-3)	4318.19
6 h	22.01 (0.54)	0.0095 (1.6 e-3)	6.57 (0.41)	8.3 e-4 (1.6 e-3)	4695.41
12 h	26.70 (0.69)	0.013 (1.7 e-3)	8.02 (0.49)	3.8 e-4 (1.6 e-3)	4722.78
24 h	31.74 (0.86)	0.022 (2.4 e-3)	8.84 (0.64)	3.8 e-3 (1.9 e-3)	4918.87
		Pluviometer Data, Climatological Network			
1 day	28.94 (0.62)	0.020 (1.9 e-3)	8.89 (0.45)	0.0017 (1.4 e-3)	22875.13
2 days	38.46 (0.86)	0.030 (3.0 e-3)	11.01 (0.72)	0.0052 (2.3 e-3)	24382.04
3 days	44.72 (0.98)	0.037 (3.7 e-3)	12.13 (0.81)	0.0073 (2.6 e-3)	24977.63
5 days	55.18 (1.26)	0.048 (4.3 e-3)	14.13 (0.80)	0.010 (3.1 e-3)	25821.24
7 days	63.45 (1.39)	0.060 (4.5 e-3)	15.48 (0.85)	0.012 (3.5 e-3)	26343.49
10 days	75.42 (1.60)	0.076 (5.9 e-3)	17.06 (0.87)	0.021 (4.2 e-3)	27181.50
15 days	91.43 (2.01)	0.094 (7.3 e-3)	20.37 (0.99)	0.024 (4.8 e-3)	28117.66
20 days	106.56 (2.45)	0.107 (8.00 e-3)	23.93 (1.33)	0.029 (5.9 e-3)	29067.82
30 days	133.47 (2.81)	0.135 (8.5 e-3)	27.90 (1.66)	0.034 (8.5 e-3)	30024.33

[a]The parameter γ is given in Table 3.

[48] This analysis can be extended in several ways. First, throughout this work it was assumed that there is no temporal dependence in the series. However, nonstationarity is often apparent in the form of trends, possibly due to long-term climate changes. Variations in time can be modeled by introducing time-dependent covariates in the GEV parameters [*Smith*, 1989; *Coles*, 2001; *Katz et al.*, 2002; *El Adlouni et al.*, 2007]. The number of papers on modeling of spatially dependent nonstationary extremes is very limited, see for example [*Northrop and Jonathan*, 2011]. In such a case, GEV parameters are time and space dependent, providing a clear view on historical changes in extremes. However, time-dependent GEV models cannot be used for practical purposes such as return period estimation. Because our project is product oriented, only stationary GEV models are considered. Secondly, seasonal effects are not accounted for, possibly due to different climate patterns in different months. Further refinement by modeling seasonal extremes would be an interesting extension of this study. Finally, the study was restricted to a limited number of durations ranging from $d = 10$ min to $d = 30$ days. It should be interesting to provide extreme rainfall intensities for any duration in the form of intensity-duration-frequency (IDF) relationships. To our knowledge, IDF curves of spatial extremes were not yet published in the literature, and might be an interesting option from which it can be hoped that it broadens the scope of the actual methodology beyond this current limitation.

Appendix A: Estimation of the Spatial Models

[49] Estimation results of $\text{GEV}_{10}^{(alt)}$, $\text{GEV}_{11}^{(alt)}$, $\text{GEV}_{10}^{(mar)}$ and $\text{GEV}_{11}^{(mar)}$ are given in Tables A1–A4.

Table A3. Estimation Results and Standard Errors for $\text{GEV}_{10}^{(mar)\,a}$

d	$\hat{\mu}_0$ (mm)	$\hat{\mu}_1$ (mm/mm)	$\hat{\sigma}$ (mm)	TIC
		Pluviograph Data, Hydrometeorological Network		
10 m	5.07 (0.43)	0.0019 (5.3 e-4)	2.59 (0.12)	3297.52
20 m	7.24 (0.50)	0.0029 (6.3 e-4)	3.82 (0.14)	3791.35
30 m	8.20 (0.65)	0.0038 (8.2 e-4)	4.66 (0.12)	4010.34
1 h	11.46 (0.76)	0.0034 (8.8 e-4)	5.20 (0.16)	4185.74
2 h	12.72 (0.89)	0.0054 (1.0 e-3)	5.87 (0.19)	4318.47
6 h	12.98 (1.39)	0.0126 (1.5 e-3)	6.64 (0.26)	4464.54
12 h	12.87 (1.57)	0.0190 (1.6 e-3)	7.91 (0.36)	4670.59
24 h	10.10 (2.09)	0.0300 (2.5 e-3)	9.27 (0.44)	4880.58
		Pluviometer Data, Climatological Network		
1 day	9.76 (1.46)	0.0251 (1.6 e-3)	8.92 (0.36)	22794.07
2 days	9.82 (2.29)	0.0376 (2.5 e-3)	11.28 (0.54)	24255.68
3 days	9.43 (2.88)	0.0463 (3.4 e-3)	12.57 (0.61)	24826.62
5 days	9.64 (3.77)	0.0600 (4.2 e-3)	14.79 (0.65)	25654.69
7 days	5.52 (3.66)	0.0761 (4.2 e-3)	16.22 (0.68)	26136.46
10 days	4.53 (4.58)	0.0935 (5.5 e-3)	18.81 (0.79)	27027.75
15 days	3.49 (6.49)	0.1159 (7.8 e-3)	22.29 (0.98)	27936.37
20 days	3.88 (7.45)	0.1352 (9.0 e-3)	26.36 (1.3)	28880.39
30 days	−0.03 (7.25)	0.1756 (8.4 e-3)	30.21 (1.9)	29772.03

[a]The parameter γ is given in Table 3.

Table A4. Estimation Results and Standard Errors for $GEV_{11}^{(mar)\,a}$

d	$\hat{\mu}_0$ (mm)	$\hat{\mu}_1$ (mm/mm)	$\hat{\sigma}_0$ (mm)	$\hat{\sigma}_1$ (mm/mm)	TIC
		Pluviograph Data, Hydrometeorological Network			
10 m	5.00 (0.65)	0.0020 (7.3 e-4)	2.00 (0.58)	6.9 e-4 (8.0 e-4)	3292.11
20 m	6.08 (0.73)	0.0042 (8.4 e-4)	1.87 (0.74)	2.2 e-4 (9.5 e-4)	3783.49
30 m	7.28 (0.92)	0.0048 (1.1 e-3)	3.02 (0.89)	0.0019 (1.1 e-3)	4005.85
1 h	9.58 (1.29)	0.0056 (1.5 e-3)	1.91 (1.20)	0.0038 (1.6 e-3)	4174.71
2 h	10.52 (1.42)	0.0080 (1.6 e-3)	2.09 (1.34)	0.0044 (1.8 e-3)	4306.55
6 h	12.38 (1.62)	0.0133 (1.8 e-3)	5.64 (1.51)	0.0011 (1.9 e-3)	4461.45
12 h	12.56 (1.80)	0.0193 (1.9 e-3)	7.30 (1.26)	7.0 e-4 (1.5 e-3)	4669.14
24 h	8.54 (2.11)	0.0319 (2.4 e-3)	5.62 (1.92)	4.2 e-3 (2.2 e-3)	4874.80
		Pluviometer Data, Climatological Network			
1 day	9.14 (1.78)	0.0259 (1.9 e-3)	7.88 (1.35)	0.0012 (1.6 e-3)	22788.09
2 days	7.71 (2.76)	0.0400 (3.1 e-3)	7.26 (1.99)	0.0047 (2.1 e-3)	24237.09
3 days	6.23 (3.22)	0.0501 (3.7 e-3)	6.35 (2.34)	0.0072 (2.6 e-3)	24794.31
5 days	4.75 (4.00)	0.0657 (4.6 e-3)	5.02 (2.51)	0.0114 (3.0 e-3)	25600.60
7 days	1.21 (4.14)	0.0812 (4.9 e-3)	5.43 (3.22)	0.0126 (3.8 e-3)	26079.42
10 days	−1.28 (4.95)	0.1003 (6.1 e-3)	0.90 (3.90)	0.0208 (4.9 e-3)	26926.34
15 days	−3.56 (6.12)	0.1242 (7.4 e-3)	1.89 (4.26)	0.0236 (5.4 e-3)	27834.72
20 days	−4.09 (6.77)	0.1445 (8.3 e-3)	0.90 (5.4)	0.0294 (6.9 e-3)	28767.38
30 days	−6.00 (7.27)	0.1822 (8.8 e-3)	4.61 (6.67)	0.0297 (8.9 e-3)	29681.32

[a]The parameter γ is given in Table 3.

References

Ailliot, P., C. Thompson, and P. Thomson (2011), Mixed methods for fitting the GEV distribution, *Water Resour. Res.*, *47*, W05551, doi:10.1029/2010WR009417.

Beirlant, J., Y. Goegebeur, J. Segers, and J. Teugels (2004), *Statistics of Extremes*, John Wiley, Hoboken, N. J.

Blanchet, J., and M. Lehning (2010), Mapping snow depth return levels: Smooth spatial modeling versus station interpolation, *Hydrol. Earth Syst. Sci.*, *14*, 2527–2544.

Blanchet, J., C. Marty, and M. Lehning (2009), Extreme value statistics of snowfall in the Swiss Alpine region, *Water Resour. Res.*, *45*, W05424, doi:10.1029/2009WR007916.

Buishand, A., and J. Wijngaard (2007), Statistiek van extreme neerslag voor korte neerslagduren, *KNMI Tech. Rep. TR-295*, K. Ned. Meteorol. Inst., De Bilt, Netherlands.

Buishand, T. A. (1983), Uitzonderlijk hoge neerslaghoeveelheden en de theorie van de extreme waarden, *Cultuurtech. Tijdschr.*, *23*, 9–20.

Buishand, T. A. (1984), Bivariate extreme-value data and the station-year method, *J. Hydrol.*, *69*, 77–95.

Buishand, T. A. (1991), Extreme rainfall estimation by combining data from several sites, *Hydrol. Sci. J.*, *36*, 345–365.

Buishand, T. A., and G. R. Demarée (1990), Estimation of the annual maximum distribution from samples of maxima in separate seasons, *Stoch. Hydrol. Hydraul.*, *4*, 89–103.

Buishand, T. A., R. Jilderda, and J. B. Wijngaard (2009), Regionale verschillen in extreme neerslag, *KNMI Sci. Rep. WR 2009-01*, K. Ned. Meteorol. Inst., De Bilt, Netherlands.

Coles, S. (2001), *An Introduction to Statistical Modeling of Extreme Values*, Springer-Verlag Heidelberg, Germany.

Cooley, D., D. Nychka, and P. Naveau (2007), Bayesian spatial modeling of extreme precipitation return levels. *J. Am. Stat. Assoc.*, *102*, 824–840.

Cunnane, C. (1973), A particular comparison of annual maxima and partial duration series methods of flood frequency prediction, *J. Hydrol.*, *18*, 257–271.

Davison, A. (2003), *Statistical Models*, Cambridge Univ. Press, Cambridge, U. K.

Delbeke, L. (2001), *Extreme neerslag in Vlaanderen: Nieuwe IDF-curven gebaseerd op langdurige meetreeksen van neerslag*, 123 pp., Minist. van de Vlaamse Gemeenschap, Afdeling Water, Brussels.

Demarée, G. R. (1985), Intensity-duration-frequency relationship of point precipitation at Uccle: Reference period 1934–1983, *Publ. Inst. R. Meteorol. Belg., Ser. A*, *116*, 52 pp.

Demarée, G. R. (2003), Le pluviographe centenaire du plateau d'Uccle: Son histoire, ses données et ses applications, *Houille Blanche*, *4*, 1–8.

Dupriez, G. L., and G. R. Demarée (1988), Contribution a l'étude des relations intensité-durée-fréquence des précipitations. Totaux pluviométriques sur des périodes continues de 1 á 30 jours. I.- Analyse de 11 séries pluviométriques de plus de 80 ans, *Misc. Ser. A, 8*, 154 pp., R. Meteorol. Inst. of Belg., Brussels.

Dupriez, G. L., and G. R. Demarée (1989), Contribution á l'étude des relations intensité-durée-fréquence des précipitations. Totaux pluviométriques sur des périodes continues de 1 30 jours. II.- Analyse des séries pluviométriques d'au moins 30 ans, *Misc. Ser. A, 8*, 53 pp., R. Meteorol. Inst. of Belg., Brussels.

El Adlouni, S., T. B. M. J. Ouarda, X. Zhang, R. Roy, and B. Bobeé (2007), Generalized maximum likelihood estimators for the nonstationary generalized extreme value model, *Water Resour. Res.*, *43*, W03410, doi:10.1029/2005WR004545.

Embrechts, P., C. Klüppelberg, and T. Mikosch (1997), *Modelling Extremal Events for Insurance and Finance*, Springer-Verlag, Berlin.

Faulkner, D. S., and C. Prudhomme (2007), Mapping of an index of extreme rainfall across the UK, *Hydrol. Earth Syst. Sci.*, *2*, 183–194.

Gellens, D. (1995), Extreme precipitation of December 1993 and January 1995 in Belgium: A homogenization procedure for estimating fractiles corresponding to long return periods, *Phys. Chem. Earth*, *20*, 451–454.

Gellens, D. (2000), Trend and correlation analysis of k-day extreme precipitation over Belgium, *Theor. Appl. Climatol.*, *66*, 117–129.

Gellens, D. (2002), Combining regional approach and data extension procedure for assessing GEV distribution of extreme precipitation in Belgium, *J. Hydrol.*, *268*, 113–126.

Gellens, D. (2003), Etude des précipitations extrêmes—Etablissement des fractiles et des périodes de retour dévénements pluviométriques, PhD thesis, 242 pp., Univ. Libre de Bruxelles, Brussels.

Hosking, J. R. M., and J. R. Wallis (1997), *Regional Frequency Analysis: An Approach Based on L-Moments*, Cambridge Univ. Press, Cambridge, U. K.

Jenkinson, A. F. (1955), The frequency distribution of the annual maximum (or minimum) values of meteorological elements, *Q. J. R. Meteorol. Soc.*, *81*, 158–171.

Katz, R. W., M. B. Parlange, and P. Naveau (2002), Statistics of extremes in hydrology, *Adv. Water Resour.*, *25*, 1287–1304.

Leadbetter, M., G. Lindgren, and H. Rootzén (1983), *Extremes and Related Properties of Random Sequences and Processes*, Springer-Verlag, New York.

Northrop, P. J., and P. Jonathan (2011), Threshold modelling of spatially dependent non-stationary extremes with application to hurricane-induced wave heights, *Environmetrics*, *22*(7), 799–809, doi:10.1002/env.1106.

Ntegeka, V., and P. Willems (2008), Trends and multidecadal oscillations in rainfall extremes, based on a more than 100 year time series of 10 min rainfall intensities at Uccle, Belgium, *Water Resour. Res.*, *44*, W07402, doi:10.1029/2007WR006471.

Overeem, A., T. A. Buishand, and I. Holleman (2008), Rainfall depth-duration-frequency curves and their uncertainties, *J. Hydrol.*, *348*, 124–134.

Overeem, A., T. A. Buishand, and I. Holleman (2009), Extreme rainfall analysis and estimation of depth-duration-frequency curves using weather radar, *Water Resour. Res.*, *45*, W10424, doi:10.1029/2009WR007869.

Ribatet, M. (2011), SpatialExtremes: An R package for modelling spatial extremes, Inst. of Math. and Modell., Univ. of Montpellier II, Montpellier, France. [Available at http://cran.r-project.org/web/packages/SpatialExtremes/.]

Robinson, M. E., and J. A. Tawn (2000), Extremal analysis of processes sampled at different frequencies, *J. R. Statist. Soc., Ser. B*, *62*, 117–135.

Smith, R. L. (1985), Maximum likelihood estimation in a class of nonregular cases, *Biometrika*, *72*, 67–90.

Smith, R. L. (1989), Extreme value analysis of environmental time series: An application to trend detection in ground-level ozone (with discussion), *Stat. Sci.*, *4*, 367–393.

Schlater, M. (2002), Models for stationary max-stable random fields, *Extremes*, *5*, 33–44.

Sneyers, R. (1960), On a special distribution of maximum values, *Mon. Weather Rev.*, *88*, 66–69.

Sneyers, R. (1975), Sur l'analyse statistique des series d'observations, *WMO Tech. Note 143*, 192 pp., World Meteorol. Org., Geneva, Switzerland.

Sneyers, R., M. Vandiepenbeeck, and R. Vanlierde (1989), Principal component analysis of Belgian rainfall, *Theor. Appl. Climatol.*, *39*, 199–204.

van Montfort, M. A. J. (1990), Sliding maxima, *J. Hydrol.*, *118*, 77–85.

van Montfort, M. A. J. (1997), Concomitants of the Hershfield factor, *J. Hydrol.*, *194*, 357–365.

Vannitsem, S., and P. Naveau (2007), Spatial dependences among precipitation maxima over Belgium, *Nonlinear Processes Geophys.*, *14*, 621–630.

Varin, C., and P. Vidoni (2005), A note on composite likelihood inference and model selection, *Biometrika*, *92*, 519–528.

Weisse, A. K., and P. Bois (2001), Topographic effects on statistical characterstics of heavy rainfall and mapping in the Frech Alps, *J. Appl. Meteorol.*, *40*, 720–740.

Wijngaard, J. B., A. M. G. Klein Tank, and G. P. Können (2003), Homogeneity of the 20th century European daily temperature and precipitation series, *Int. J. Climatol.*, *23*, 679–692.

Willems, P. (2000), Compound intensity/duration/frequency-relationships of extreme precipitation for two seasons and two storm types, *J. Hydrol.*, *233*, 189–205.

Witter, J. V. (1984), Heterogeneity of Dutch rainfall, PhD thesis, 204 pp., Wageningen Univ., Wageningen, Netherlands.